Laminar flame speeds of DMF/ Iso -octane-Air-N 2/CO 2 mixtures

ARTICLE *in* ENERGY & FUELS · FEBRUARY 2012

Impact Factor: 2.79 · DOI: 10.1021/ef201638w

5 AUTHORS, INCLUDING:

Qianqian Li
Xi'an Jiaotong University
26 PUBLICATIONS **450** CITATIONS
SEE PROFILE

Jin Fu
Xi'an Jiaotong University
16 PUBLICATIONS **132** CITATIONS
SEE PROFILE

Chenglong Tang
Xi'an Jiaotong University
72 PUBLICATIONS **740** CITATIONS
SEE PROFILE

Zuohua Huang
Xi'an Jiaotong University
421 PUBLICATIONS **5,195** CITATIONS
SEE PROFILE

energy&fuels

Article

pubs.acs.org/EF

Laminar Flame Speeds of DMF/*iso*-octane-Air-N_2/CO_2 Mixtures

Qianqian Li, Jin Fu, Xuesong Wu, Chenglong Tang, and Zuohua Huang*

State Key Laboratory of Multiphase Flow in Power Engineering, Xi'an Jiaotong University, Xi'an, People's Republic of China

ABSTRACT: Laminar combustion characteristics of 2,5-dimethylfuran (DMF)/*iso*-octane/air/diluent (15% N_2/85% CO_2) mixtures at atmospheric pressure and the initial temperature of 393 K were studied using the outwardly propagating spherical flame and high speed schlieren photography. Effects of DMF concentration in the fuel mixture and dilution ratio on flame properties were investigated, such as laminar flame speed, adiabatic temperature, effective Lewis number, and laminar flame thickness. Results show that laminar flame speed varied little, while the flame instability was slightly promoted as DMF concentration in the blends is increased. For all the fuels at fixed equivalence ratio, flame front morphology showed that the flame stability was enhanced with increasing dilution ratio. In addition, a linear relationship between the normalized laminar flame speed and the dilution ratio was found and an empirical formula was proposed for all the four different fuels at different equivalence ratios.

1. INTRODUCTION

To meet the requirements of energy saving in the face of energy shortage and increasingly stringent environment regulations, many studies have been done on finding the promising alternative fuels for gasoline. 2,5-Dimethylfuran (DMF), for instance, is a second-generation biofuel and has several advantages compared to other alternatives, such as ethanol. DMF is water insoluble, and its energy density is closer to that of gasoline; DMF has a higher boiling point than that of ethanol and has a high octane number. DMF can be produced on a large scale from cellulose and sugar,[1,2] and production of DMF consumes two-thirds less energy than production of ethanol.[3] Because of the described features of DMF, it is regarded as one of the most promising candidates as a substitute for gasoline, and practically, considerable work on DMF-fueled engines has been also conducted. Zhong et al.[4] investigated the performance of a gasoline direct-injection spark-ignition engine fueled by DMF, and their results showed DMF's performance was, if not better, at least comparable to that of gasoline. Daniel et al.[5] conducted experiments on a single-cylinder spark-ignition engine and found that DMF had a faster burning rate and shorter initial combustion duration than gasoline, and in addition, the thermal efficiency of the engine fueled with DMF was higher than that of gasoline. Wu et al.[6] investigated effects of the flexible dual injection of gasoline/DMF and gasoline/ethanol on a spark-ignition engine performance. Results showed the gasoline/DMF had shorter combustion duration and fewer HC emissions but higher NO_x and CO_2 emissions, as compared to gasoline/ethanol. Fundamentally, the combustion characteristics of DMF have not been sufficiently studied. Wu et al.[7,8] measured the laminar burning velocities and Markstein length of DMF/air mixtures at elevated temperatures and pressures. Wu et al.[9] also studied the low-pressure premixed laminar 2,5-dimethylfuran/oxygen/argon flame with tunable vacuum ultraviolet synchrotron radiation photoionization and molecular-beam mass spectrometry, and possible reaction pathways were proposed.

Laminar combustion information is the benchmark of turbulent combustion. Laminar flame speed is a physiochemical property that characterizes the reactivity, exothermicity, and diffusivity of a combustible mixture, and it has been constantly used for the developing and validating of the chemical kinetics.[10,11] The understanding of flame instabilities will help the analysis of engine performance and emission.[12,13] Laminar combustion research is carried out using the spherically propagating flame.[14,15]

Practically, EGR (exhaust gas recirculation) is constantly used in diesel engine to decrease the combustion temperature and thus NO_x emissions. In the spark-ignition engine, EGR is also a flexible technique that could reduce the pumping losses at partial load and improve the detonation resistance at full load, besides decreasing the of NO_x emissions.[16] From a fundamental combustion point of view, much work on EGR simulants has been conducted. As the main components in EGR are nitrogen and carbon dioxide, much work on nitrogen and carbon dioxide as diluents has been conducted. Halter et al.[17] studied the impact of different diluents on the laminar flame speeds of two different fuels (methane and *iso*-octane), and the diluents include nitrogen, carbon dioxide, and the mixture of 71.6% nitrogen and 28.4% carbon dioxide. Tran Manh et al.[18] studied the influence of the diluents nitrogen and carbon dioxide on flame cellular instabilities of syngas and found that Markstein length of CO_2-diluted and N_2-diluted syngas/air mixture decrease with the increase of dilution ratio. Far et al.[19] studied the effect of diluents (14% CO_2 and 86% N_2) on flame structure and laminar flame speeds of JP8/oxidizer/diluent premixed flame at high temperatures and pressures and found that the addition of diluents decreased the laminar flame speed and had little influence on the flame stability. Wu et al.[20] used nitrogen and carbon dioxide as diluents of the DMF/air mixture and gave the variations of laminar flame speed and flame stability with the dilution ratio.

In this study, the EGR simulant is composed of 15% carbon dioxide and 85% nitrogen, whose thermodynamic properties

Received: October 22, 2011
Revised: December 23, 2011
Published: December 26, 2011

   dx.doi.org/10.1021/ef201638w | *Energy Fuels* 2012, 26, 917–925

are close to that of typical engine exhaust gases. *Iso*-octane is used to simulate gasoline, and DMF is a fuel octane number improver. The objective of the study is to investigate laminar flame speeds and flame instabilities of diluted DMF/*iso*-octane fuel mixtures with different blending ratios and dilution ratios. The physical parameters of DMF and *iso*-octane are listed in Table 1. The four kinds of fuel blends are designated as D00, D10, D20, and D30, respectively (vol. DMF/*iso*-octane: 00/100, 10/90, 20/80, and 30/70).

Table 1. Physical Parameters of Fuels[32,39,40]

	DMF	ethanol	*iso*-octane
chem. formula	C_6H_8O	C_2H_6O	C_8H_{18}
comp. (C/H/O) (mass %)	75/8.3/16.7	52.2/13/34.8	84/16/0
molar mass (g/mol)	96.13	46.07	114.23
lower heating value (MJ/kg)	42	26.8	42.7
density (kg/m^3)	900	789	688
octane number	119	129	100
melting point (°C)	−62	−114	−107.38
boiling temp. (°C)	92−94	78	99.3
latent heat of vaporization (kJ/mol)	31.91	41.65	32.327
self-ignition temp. (°C)	285.85	422	417
stoichiometric air/fuel ratio	10.72	8.95	15.13
mixture calorific value (MJ/kg)	33.7	26.9	43.2
solubility in water at 20 °C (mL/100 mL H_2O)	insoluble <1 mg/mL	miscible	immiscible

2. EXPERIMENTAL SETUP AND PROCEDURES

2.1. Experimental Setup. Details of the experimental apparatus can be seen in previous papers,[20,21] and here, we only give a brief introduction. The whole system includes the high-speed digital camera (HG-100K, American Redlake Corporation), the combustion chamber, the ignition circuit, the pressure date acquisition system, the mixture preparation manifold, and the control circuits. The chamber is equipped with a pressure transmitter and a thermocouple to measure the pressure and temperature. In this experiment, the initial pressure is atmospheric pressure, and the pressures of the components are measured with mercury manometer. Two quartz windows are mounted on each side of the chamber, allowing for optical access. Two electrodes are located centrally to ignite the mixture. The purity levels of the liquid fuel and the gas used here are over 99%. The air used in the experiments is the mixture of 21% O_2 and 79% N_2 in volume. Dilution ratio is defined as

$$\varphi_r = \frac{V_{\text{diluent}}}{V_{\text{diluent}} + V_{\text{fuel}} + V_{\text{air}}} \quad (1)$$

The initial temperature is identified to be 393 K to ensure the fuels to be fully vaporized. The equivalence ratio is over the range 0.9−1.5. When the mixture is heated to the initial temperature, the calculated liquid mixed fuel corresponding to the fixed condition can be injected into the chamber using the microliter syringes. After waiting 6 or 8 min, the mixture is ignited, and meanwhile, the camera starts to record the flame propagation phenomenon. For each operating condition, the experiment is repeated at least three times to ensure the accuracy.

2.2. Data Processing. The raw data obtained directly through experiments is the flame radius history $r_f(t)$, through which the flame propagation speed can be evaluated by $S_b = dr_f/dt$. The overall stretch rate, $\kappa = (2/r_f)S_b$, can be linearly correlated with S_b (i.e. $S_b^0 - S_b = L_b\kappa$).[22] Through linear regression, the unstretched propagating speed S_b^0 and Markstein length L_b, with respect to the burned gases, can be obtained (shown in Figure 4a). The laminar flame speed with respect to the unburned gases can be evaluated through continuity across the flame front, $S_u^0 = \rho_b^0 S_b^0/\rho_u$. Here, we define the flame thickness as $l_f = \nu/S_u^0$, where ν is the kinematic viscosity of the unburned mixture. The burned gas thermal data were obtained by thermal equilibrium calculation.

Laminar flame speed calculations were performed using the Chemkin Premix code[23] with detailed chemistry and transport. The chemical mechanism used here is the PRF model developed by Chaos et al.[24]

2.3. Mechanism of Flame Front Instability. There are three mechanisms responsible for flame front instabilities: the buoyancy instability, which becomes significant when the flame speed is low enough (typically for flame near lean flammability limit); the intrinsic hydrodynamic instability, which is caused by the density jump across the flame under the assumption of infinitely thin flame;[25,26] and the diffusional-thermal instability, which is caused by the nonequal diffusion between heat and mass.[27−29] In this work, flames near the flammability limit were not studied, thus the buoyancy-driven instability is neglected. The hydrodynamic instability affects the flame pattern dramatically when the pressure is high because the minimized flame thickness shifts the situation more closer to Landau's zero flame thickness assumption,[29] thus this mechanism is not the focus of this work because we studied the flame front pattern at 0.1 MPa. The diffusional-thermal instability could be quantified by the Lewis number, *Le*, which is defined as the ratio of the mixture thermal diffusivity and the mass diffusivity.[30,31] In a fuel mixture/air system, an effective Lewis number, which is the weighted average of the specific fuel Lewis number, should be used to characterize the overall nonequal diffusion behavior.

The approach of Law et al.[30] was adopted here to calculate the following:

$$Le_{\text{eff}} = 1 + \frac{q_{\text{DMF}}(Le_{\text{DMF}} - 1) + q_{\text{iso}}(Le_{\text{iso}} - 1)}{q} \quad (2)$$

where q_{DMF} and q_{iso} are the nondimensional heat release for the consumption of species, $q = q_{\text{DMF}} + q_{\text{iso}}$. Le_{DMF} and Le_{iso} are the Lewis number of DMF at ϕ_{DMF} and *iso*-octane at ϕ_{iso}, respectively.

3. RESULTS AND DISCUSSIONS

3.1. System Validation. The error analysis of the experimental setup and methods for liquid fuel has been conducted in a previous study by Gu et al.[32] To further validate our experimental apparatus, the laminar flame speed of the *iso*-octane/air mixtures at the pressure of 1 atm and temperature of 393 K were measured and compared with previously published results, as shown in Figure 1. The work of Mounaim-Rousselle et al.[33] was conducted at the same initial conditions as the present work, while the work of Kumar et al.[34] was at a temperature of 400 K. It is seen that all the laminar flame speeds peak at the

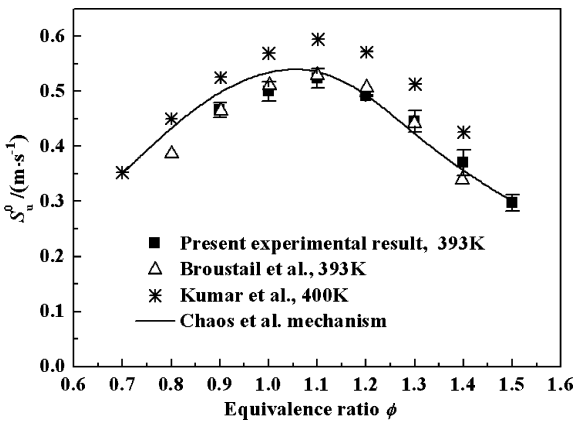

Figure 1. Laminar flame speeds versus equivalence ratio.

dx.doi.org/10.1021/ef201638w | *Energy Fuels* 2012, 26, 917−925

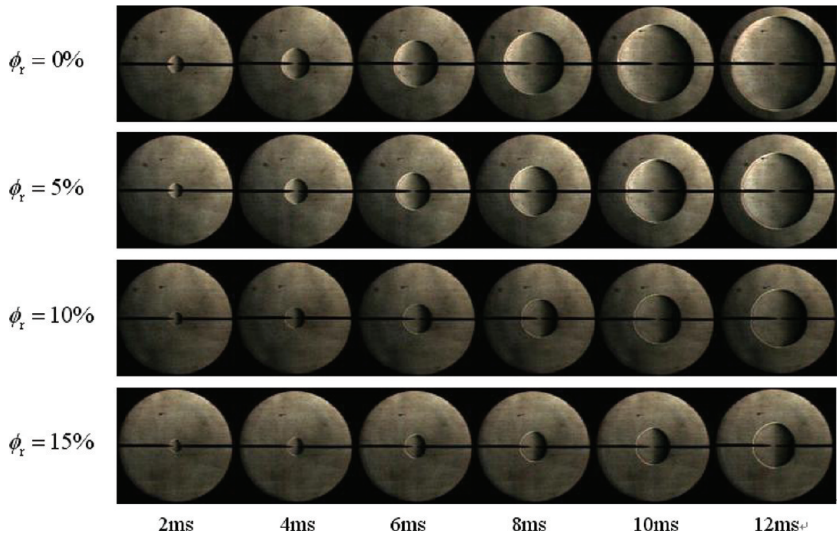

Figure 2. Schlieren images of the DMF/*iso*-octane-N_2/CO_2 mixtures at equivalence ratio of 1.2.

equivalence ratio of 1.1. Good agreement between the measurements of Mounaim-Rousselle et al. and the present work was observed. The simulated laminar flame speeds using the mechanism of Chaos et al. are in good agreement with the present measurements for rich mixtures and slightly bigger, but also very close, for lean mixtures. The data of Kumar et al. is a little higher than our measurements because they conducted their measurements at a slightly higher temperature. The good agreement between our results and previously measured and calculated flame speeds of *iso*-octane/air verifies that our apparatus is applicable for laminar flame speed measurements.

3.2. Laminar Flame Speed and Adiabatic Flame Parameters. Only the raw data with flame radius ranging between 6 mm and 25 mm was selected for further analysis, in order to exclude the effects of spark ignition, pressure rise and system confinement.[20,29,35−37] Figure 2 shows the schlieren images of the diluted D20 flames at the equivalence ratio of 1.2 and for different dilution ratios. A smooth flame front is maintained during the recorded process in which the flame ball grows. At the same time point after ignition, the flame radius is progressively smaller with increasing dilution ratio. Figure 3

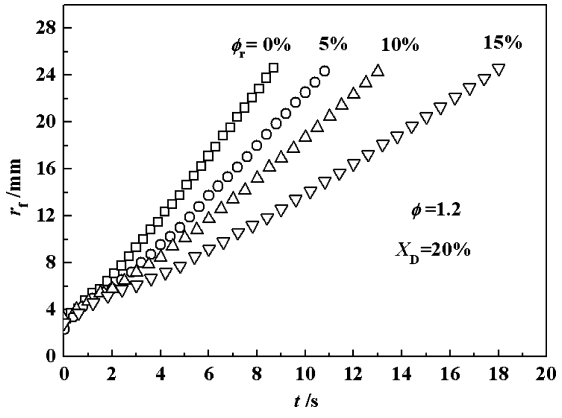

Figure 3. Flame radius versus time at different dilution ratios.

shows the history of the flame radius in Figure 2. The radius varies almost linearly with the time, except for the very beginning stage where the flame propagation is affected by electrode cooling, the spark ignition energy, the unsteady transition, and the high stretch rate. With the increase of dilution ratio, flame radius grows slower.

In Figure 4, the stretched flame propagation speeds versus stretch rates were plotted for parts a, b, and c, different fuels with no dilution at the equivalence ratio of 0.9, 1.2, 1.5, respectively, and for part d, D30 fuel with increasing dilution ratio. Here, we define X_D as the DMF mixing ratio in the blends. For all the cases shown here, the stretched flame propagation speeds decrease almost linearly with increasing stretch rates. In Figure 4a−c, the stretched flame speeds are gradually increasing, while the slopes increase and L_b values decrease with the increase of X_D. L_b, Markstein length, reflects the instability of flame and characterizes the effect of the stretch on flame propagation. A positive L_b indicates a stable flame while a negative L_b indicates an unstable flame. Greater L_b means a more stable flame front. Thus, the flame front instability will be slightly enhanced with the increase of X_D. Although the relationship between stretched flame speed and stretching rate at the equivalence of 1.5 is not as obvious as at 0.9 and 1.2, it still can be observed. Figure 4d shows that the stretched and unstretched flame speeds of one fuel for a fixed equivalence ratio all decrease with the increase of the dilution ratio. There are two reasons for this. One is the dilution effect. The dilution addition could decrease the oxygen and the fuel concentration per unit volume, and the total heat release from chemical reaction decreases. The other is the absorption of heat. Diluents will absorb part of the released heat from the combustion, and this decreases the combustion temperature, which will further decrease the flame speed. The temperature variation can be reflected by the adiabatic flame temperature.

Figure 5a gives the stretch-free laminar flame speed of *iso*-octane/DMF/air mixtures as a function of X_D for different equivalence ratios. The error bars represent the deviation of the measured data from the repeated experimentations. An interesting phenomenon observed is that the laminar flame speed is almost constant with increasing X_D. To some extent this is a good thing because the constant laminar flame speed with variation of in the extent of DMF addition favors the compatibility of DMF with oxygenated additives. Figure 5b shows the stretch-free laminar flame speed of *iso*-octane/DMF/air/diluents as a function of the dilution ratio. For given mixture

dx.doi.org/10.1021/ef201638w | *Energy Fuels* 2012, 26, 917−925

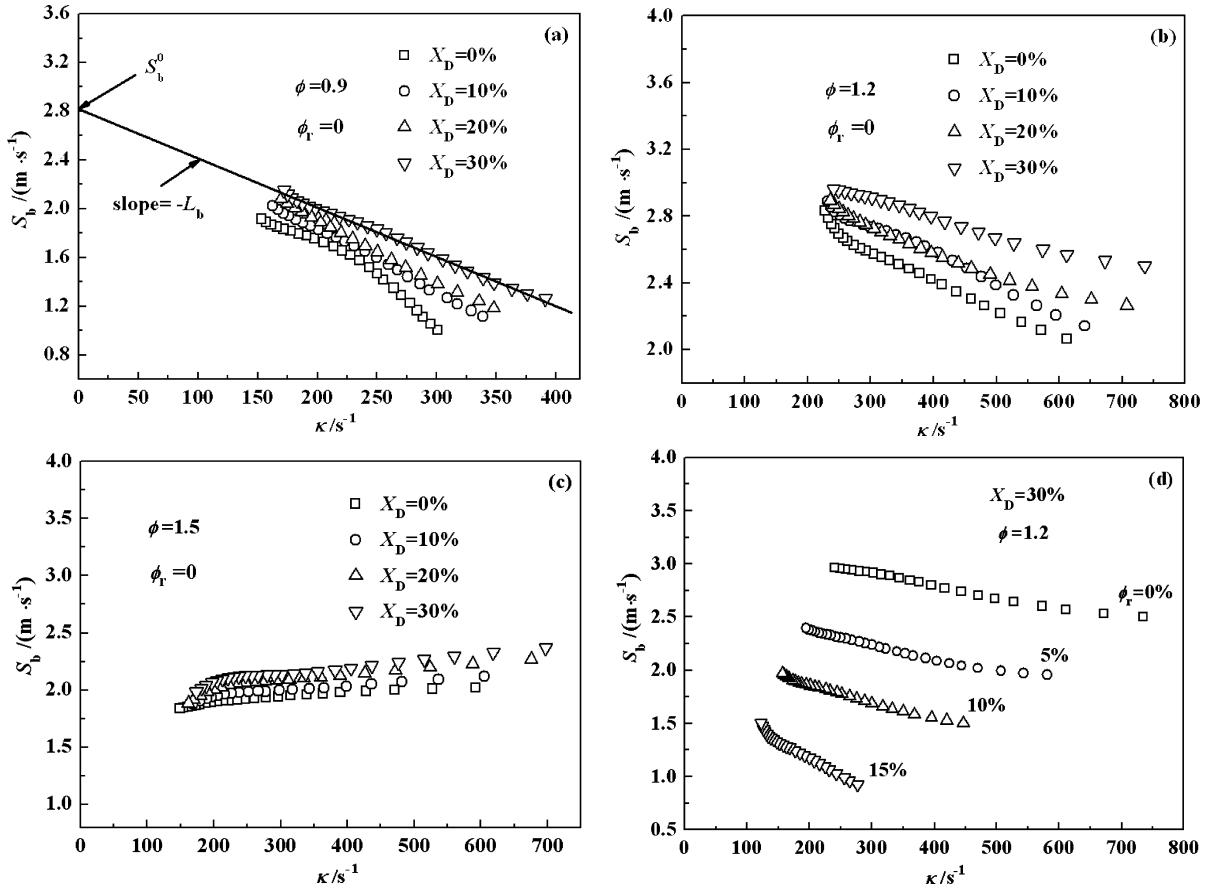

Figure 4. Stretched flame speed versus stretch rate at different DMF rations: (a) ϕ = 0.9; (b) ϕ = 1.2; and (c) ϕ = 1.5. (d) Stretched flame speed versus stretch rate at different dilution ratios.

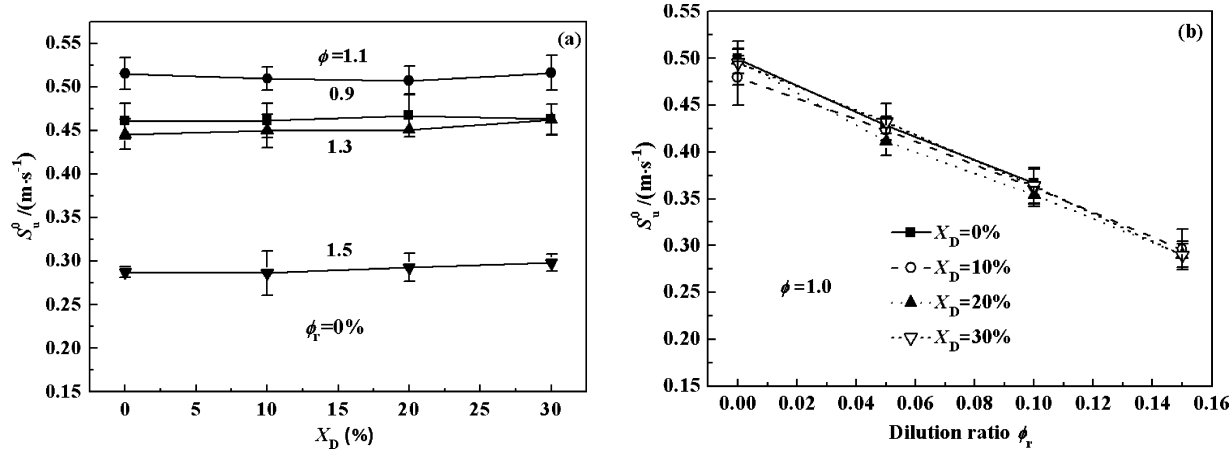

Figure 5. Unstretched flame speed as function of DMF ratio (a) and dilution ratio (b).

stoichiometry, the laminar flame speed decreases linearly with dilution ratio.

Figure 6a shows the adiabatic flame temperature, T_{ad}, as a function of X_D for different equivalence ratios. For given equivalence ratio, T_{ad} increases slightly with increasing DMF concentration, and T_{ad} attains the highest value at the equivalence ratio 1.1, among all equivalence ratios. Figure 6b shows the adiabatic flame temperature, T_{ad}, versus the dilution ratio for different fuels. T_{ad} decreases significantly with the increase of the dilution ratio for the fixed fuel.

Figures 7 and 8 show the density ratio and flame thickness at different conditions, respectively. For *iso*-octane/DMF/air mixtures, the density ratio does not largely vary when X_D increases, and the flame thickness follows the same rule for most equivalence ratios, except 1.5. The reason for this might be that, at the extremely rich case, the addition of DMF increases the oxygen concentration in the fuel blends, which facilitates the reaction under rich cases, as evidenced by the slight increase in flame speed shown in Figure 5a. Additionally, the kinematic viscosity decreases slightly more remarkably at the equivalence ratio of 1.5 than the case for 0.9, 1.1, and 1.3. However, this is

dx.doi.org/10.1021/ef201638w | *Energy Fuels* 2012, 26, 917−925

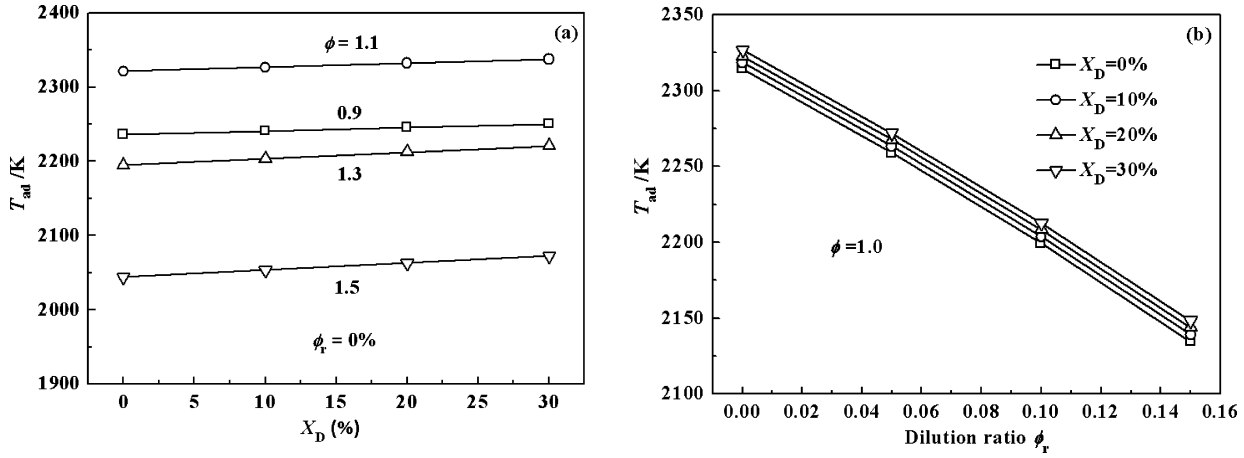

Figure 6. Adiabatic flame temperature as function of DMF ratio (a) and dilution ratio (b).

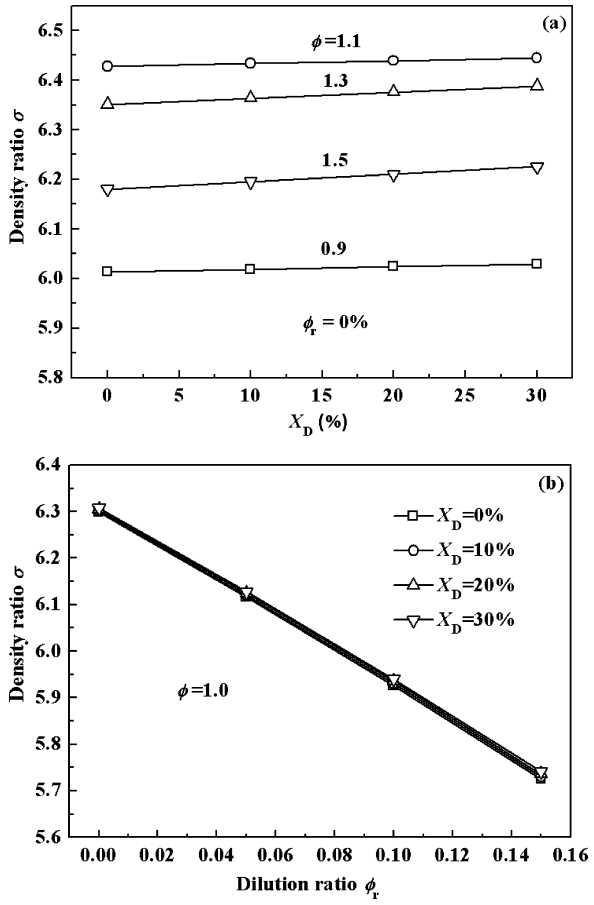

Figure 7. Density ratio as function of DMF ratio (a) and dilution ratio (b).

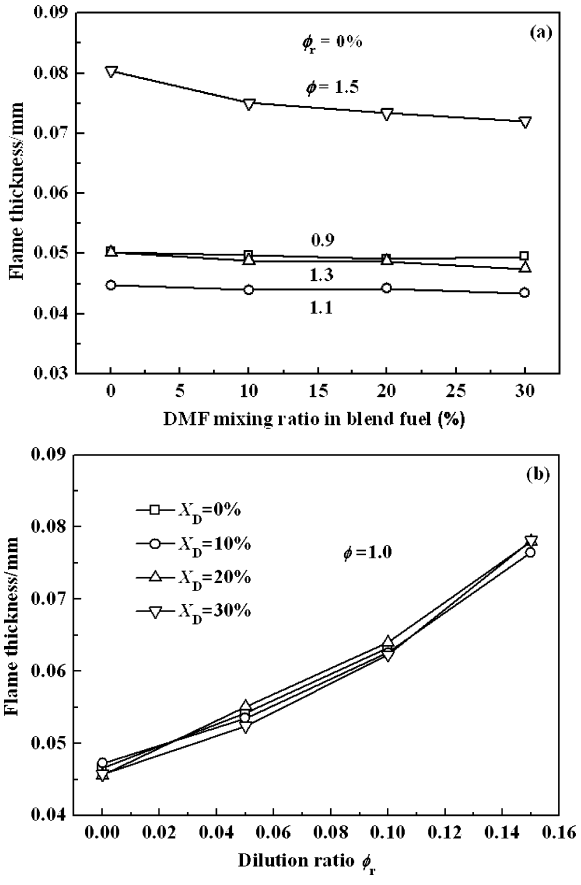

Figure 8. Flame thickness as function of DMF ratio (a) and dilution ratio (b).

just speculation, and kinetic model is needed to address this problem. Meanwhile, the density ratio decreases and the flame thickness increases obviously with the increase of the dilution ratio for the fixed fuel and given equivalence ratio. Therefore, the hydrodynamic instability is suppressed with the increasing dilution ratio.

3.3. Effective Lewis Number and Flame Morphology. Figure 9 shows the effective Lewis number (Le_{eff}) versus the dilution ratio for the four fuels at lean and rich conditions. At the equivalence ratio of 0.9, Le_{eff} decreases with the increase of dilution ratio; at the equivalence ratio of 1.1 and 1.3, the Lewis number is insensitive to the variation of dilution ratio; and at the equivalence ratio of 1.5, the effective Lewis number increases slightly with the increase of dilution ratio. No matter what the condition is, the effective Lewis number varies little. It is noted that, when evaluating the Lewis number, we should always select the mass diffusivity of the deficient species, and the mass diffusivity has a significant decrease from lean mixture to rich mixture. Figure 10 shows the effective Lewis number versus the equivalence ratio for different fuels with no dilution. Le_{eff} decrease monotonically with the increase of equivalence

dx.doi.org/10.1021/ef201638w | Energy Fuels 2012, 26, 917–925

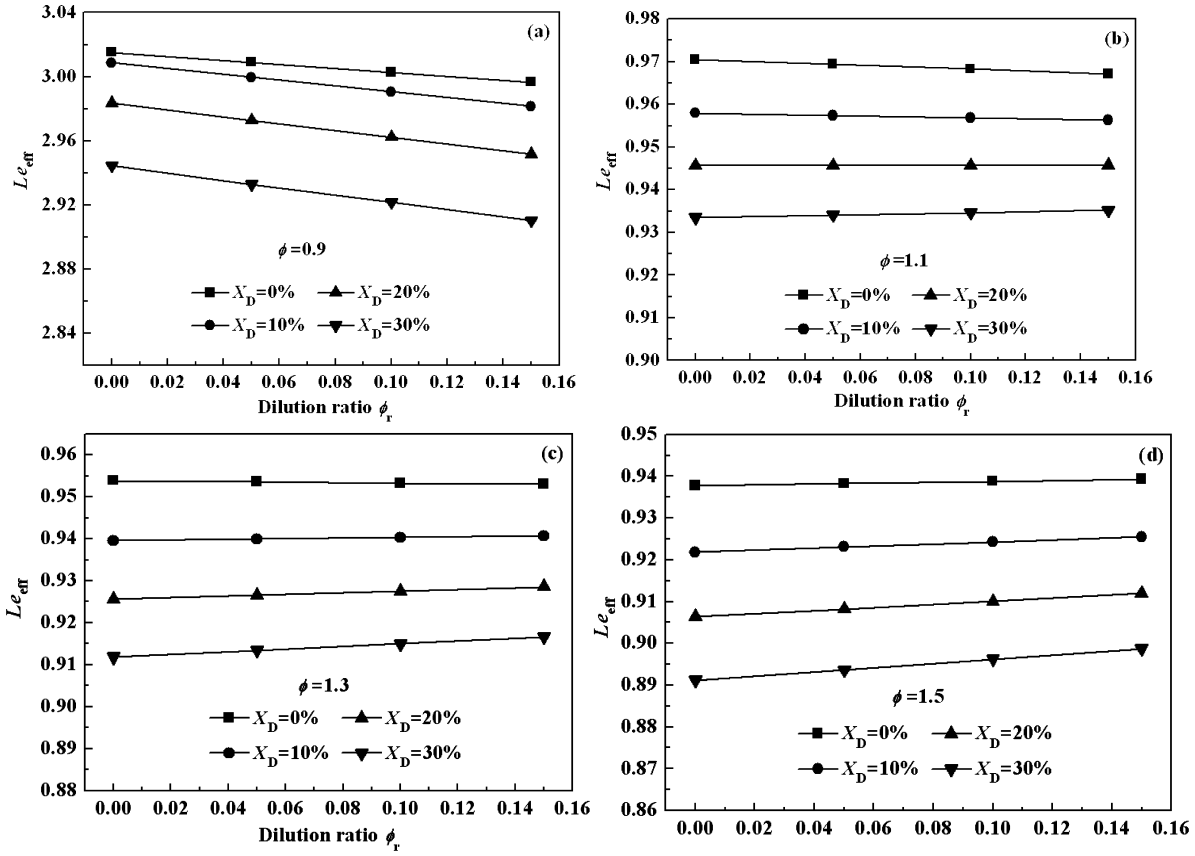

Figure 9. Lewis number versus dilution ratio at different equivalence ratios: (a) ϕ = 0.9; (b) ϕ = 1.1; (c) ϕ = 1.3; and (d) ϕ = 1.5.

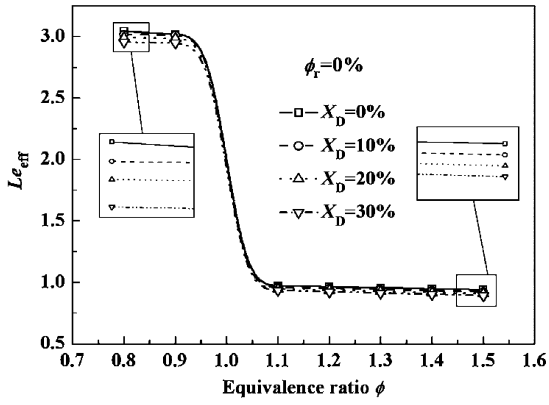

Figure 10. Lewis number versus equivalence ratio for different fuels.

ratio and illustrates that diffusional-thermal instability is enhanced. When the equivalence ratio and the dilution ratio are certain, Le_{eff} decreases when X_D increases. This indicates that DMF addition will promote the diffusional-thermal instability.

Figure 11 (top) shows the schlieren images of the expanding spherical flame using fuel mixture of D20 at four different equivalence ratios, and Markstein length and Lewis number are tabulated at the right side of the photos. The flame front at a stoichiometric ratio 0.9 or 1.1 maintains a smooth surface, and this denotes that the flame front is stable. There are always perturbations on the flame front resulting from the electrodes and spark energy at 1.3, but can be stabilized by the flame stretch and the thermodiffusion effect. When the mixture is rich, at a stoichiometric ratio of 1.5, the flame stretch and the thermodiffusion effect will not stabilize the flame or even destabilize the flame front, thus cracks appeared on the flame front and develop more and the flame becomes unstable. Markstein lengths for the equivalence ratios of 0.9, 1.1, 1.3 are positive, which indicate a stable flame, while it is negative for 1.5, which indicates an unstable flame front. The results are in good agreement with the pictures and show the rationality of using the Markstein length to explain the variation of flame instability. Le_{eff} decreases monotonically with the increase of the equivalence ratio and shows that the diffusional-thermal instability plays an important role in the variation of flame instability.

Figure 11 (bottom) shows the images of the expanding spherical flame of *iso*-octane/DMF/air mixtures at the equivalence ratio of 1.5. Regardless of fuel type, cracks can be observed on the flame front for different fuels when flame radius exceeds 20 mm. That is because the fuel mixture is rich and DMF and *iso*-octane are heavy hydrocarbons. However, obvious differences could not be observed from the images for different fuels. This result is not contradicted with the previous conclusion that the flame instability is promoted when X_D increases and that differences are not obvious the images. Actually, the result is in agreement with the conclusion that the Markstein length is negative and varies little.

3.4. Normalization and Empirical Correlation. Finally, the laminar flame speed of the DMF/*iso*-octane/air/diluents mixtures at various equivalence ratios, $S_b^0(\phi_r, \phi, X_D)$, were normalized with the laminar flame speed $S_b^0(0, \phi, X_D)$. When we plot the data for different DMF concentration at different equivalence ratios, as shown in Figure 12, all the curves are merged into a simple line.

dx.doi.org/10.1021/ef201638w | *Energy Fuels* 2012, 26, 917–925

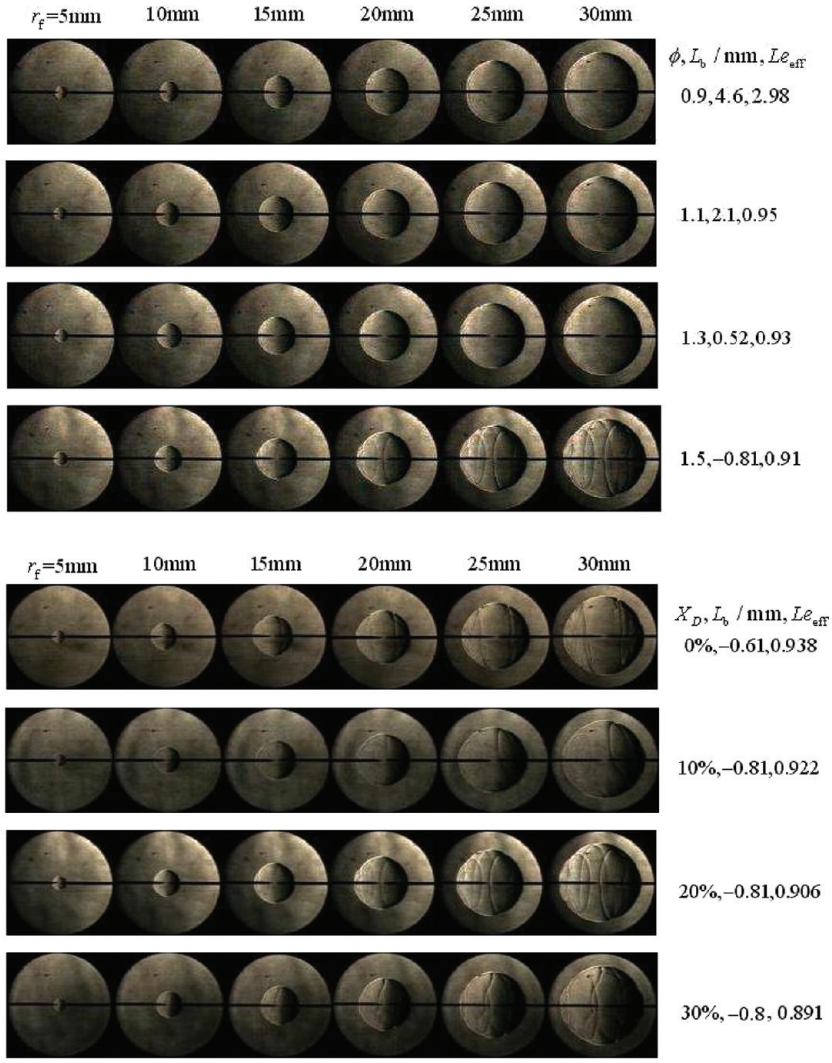

Figure 11. Schlieren images of flames: (top) D20 mixtures at different equivalence ratios without dilution; (bottom) four kinds of mixtures at an equivalence ratio of 1.5 without dilution.

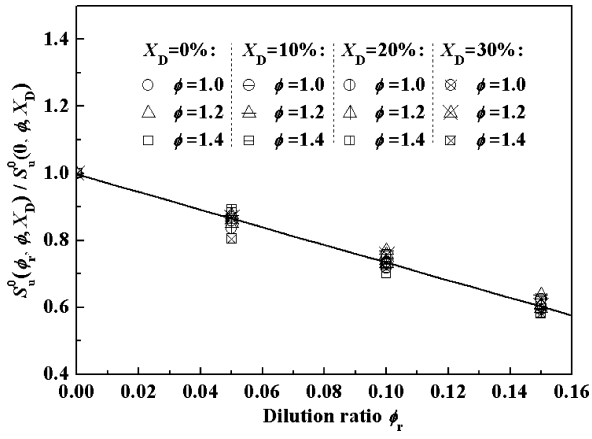

Figure 12. Normalized laminar flame speeds versus dilution ratio at different equivalence ratios for different fuels.

$$\frac{S_b^0(\varphi_r, \varphi, X_D)}{S_b^0(0, \varphi, X_D)} = a\varphi_r + b \tag{3}$$

where $a = -2.63$ and $b = 1.00$, and $S_b^0(0, \phi, X_D)$ refers to the laminar flame speed of each fuel without diluents. Previous studies have suggested that diluent has the same effect on laminar flame speed at all equivalence ratios for a given dilution ratio.[20,21,38] The study in this paper also follows the rule. Besides, it can be concluded that the extent of the dilution effect acting upon the laminar flame speeds of DMF/*iso*-octane fuels is independent of the blending ratio.

4. CONCLUSIONS

Laminar combustion characteristics of DMF/*iso*-octane/N_2/CO_2/air mixture were studied. The main conclusions are summarized as follows:

1. For a fixed equivalence ratio without dilution, the laminar flame speed varies little while the flame instability is promoted slightly according to the order of D00, D10, D20, D30, which indicates that DMF has potential as a replacement for or as an additive to gasoline.
2. For a specified fuel and a certain equivalence ratio, with the increase of the dilution ratio, the laminar flame speed decreases monotonically and almost linearly; Lewis number varies little while the density ratio decreases and the flame thickness increases obviously, which indicate that diffusional-thermal instability is largely unaffected and that hydrodynamic instability is suppressed.

dx.doi.org/10.1021/ef201638w | *Energy Fuels* 2012, 26, 917–925

3. The normalized flame speed varies little no matter the equivalence ratio or the fuel type, and a linear correlation between the normalized laminar flame speed and dilution ratio is presented, which is independent of the equivalence ratio and the DMF mixing ratio in the DMF/*iso*-octane blends.

AUTHOR INFORMATION

Corresponding Author

*Telephone: 0086-29-82665075. Fax: 0086-29-82668789. E-mail: zhhuang@mail.xjtu.edu.cn.

ACKNOWLEDGMENTS

This work is supported by the National Natural Science Foundation of China (Grant Nos. 51136005 and 50876085).

REFERENCES

(1) Mascal, M.; Nikitin, E. B. Direct, high-yield conversion of cellulose into biofuel. *Angew. Chem., Int. Ed.* **2008**, *47* (41), 7924−7926.

(2) Zhao, H.; Holladay, J. E.; Brown, H.; Zhang, Z. C. Metal chlorides in ionic liquid sovlents convert sugars to 5-hydroxymethylfuran. *Science* **2007**, *5831*, 1597−1600.

(3) Tian, G. H.; Daniel, R.; Li, H. Y.; Xu, H. M.; Shuai, S. J.; Richards, P. Laminar burning velocities of 2,5-dimethylfuran compared with ethanol and gasoline. *Energy Fuels* **2010**, *24*, 3898−3905.

(4) Zhong, S. H.; Daniel, R.; Xu, H.; Zhang, J.; Turner, D.; Wyszynski, M. L.; Richards, P. Combustion and emissions of 2,5-dimethylfuran in a direct-injection spark-ignition engine. *Energy Fuels* **2010**, *24*, 2891−2899.

(5) Daniel, R.; Tian, G. H.; Xu, H. M.; Wyszynski, M. L.; Wu, X. S.; Huang, Z. H. Effect of spark timing and load on a DISI engine fuelled with 2,5-dimethylfuran. *Fuel* **2011**, *90* (2), 449−458.

(6) Wu, X. S.; Daniel, R.; Tian, G. H.; Xu, H. M.; Huang, Z. H.; Richardson, D. Dual-injection: The flexible, bi-fuel concept for spark-ignition engines fuelled with various gasoline and biofuel blends. *Appl. Energy* **2011**, *88* (7), 2305−2314.

(7) Wu, X. S.; Huang, Z. H.; Jin, C.; Wang, X. G.; Wei, L. X. Laminar burning velocities and Markstein lengths of 2,5-dimethylfuran-air premixed flames at elevated temperatures. *Combust. Sci. Technol.* **2011**, *183*, 220−237.

(8) Wu, X. S.; Huang, Z. H.; Wang, X. G.; Jin, C.; Tang, C. L.; Wei, L. X.; Law, C. K. Laminar burning velocities and flame instabilities of 2,5-dimethylfuran−air mixtures at elevated pressures. *Combust. Flame* **2011**, *158*, 539−546.

(9) Wu, X. S.; Huang, Z. H.; Yuan, T.; Zhang, K. W.; Wei, L. X. Identification of combustion intermediates in a low-pressure premixed laminar 2,5-dimethylfuran-oxygen-argon flame with tunable synchrotron phoinization. *Combust. Flame* **2009**, *156*, 1365−1376.

(10) Bradley, D.; Hicks, R. A.; Lawes, M.; Sheppard, C. G. W.; Woolley, R. The measurement of laminar burning velocities and Markstein numbers for *iso*-octane−air and *iso*-octane−*n*-heptane−air mixtures at elevated temperatures and pressures in an explosion bomb. *Combust. Flame* **1998**, *115* (1−2), 126−144.

(11) Pareja, J.; Burbano, H. J.; Ogami, Y. Measurements of the laminar burning velocity of hydrogen−air premixed flames. *Int. J. Hydrogen Energy* **2010**, *35* (4), 1812−1818.

(12) Heywood, J. B. *Internal Combustion Engine Fundamentals*; McGraw-Hill Inc.: New York, 1988.

(13) Glassman, I. *Combustion*; Academic Press: New York, 1977.

(14) Tang, C. L.; Huang, Z. H.; Jin, C.; He, J. J.; Wang, J. H.; Wang, X. B.; Miao, H. Y. Laminar burning velocities and combustion characteristics of propane-hydrogen-air premixed flames. *Int. J. Hydrogen Energy* **2008**, *33* (18), 4906−4914.

(15) Tseng, L. K.; Ismail, M. A.; Faeth, G. M. Laminar burning velocities and Markstein numbers of hydrocarbon/air flames. *Combust. Flame* **1993**, *95* (4), 410−426.

(16) Fontana, G.; Galloni, E. Experimental analysis of a spark-ignition engine using exhaust gas recycle at WOT operation. *Appl. Energy* **2010**, *87* (7), 2187−2193.

(17) Halter, F.; Foucher, F.; Landry, L.; Mounaim-Rousselle, C. Effect of dilution by nitrogen and/or carbon dioxide on methane and *iso*-octane air flames. *Combust. Sci. Technol.* **2009**, *181* (6), 813−827.

(18) Tran Manh, V.; Jeong, P.; Oh Boong, K.; Dae Seok, B.; Jin Han, Y.; Sang In, K. Effects of diluents on cellular instabilities in outwardly propagating spherical syngas−air premixed flames. *Int. J. Hydrogen Energy* **2010**, 3868−80.

(19) Far, K. E.; Moghaddas, A.; Metghalchi, H.; Keck, J. C. The effect of diluent on flame structure and laminar burning speeds of JP-8/oxidizer/diluent premixed flames. *Fuel* **2011**, *90*, 1476−1486.

(20) Wu, X. S.; Huang, Z. H.; Jin, C.; Wang, X. G.; Zheng, B.; Zhang, Y. J.; Wei, L. X. Measurements of laminar burning velocities and Markstein lengths of 2,5-dimethylfuran-air-diluent premixed flames. *Energy Fuels* **2009**, *23*, 4355−4362.

(21) Zhang, X.; Huang, Z. H.; Zhang, Z. Y.; Zheng, J. J.; Yu, W.; Jiang, D. M. Measurements of laminar burning velocities and flame stability analysis for dissociated methanol−air−diluent mixtures at elevated temperatures and pressures. *Int. J. Hydrogen Energy* **2009**, *34* (11), 4862−4875.

(22) Gu, X. J.; Haq, M. Z.; Lawes, M.; Woolley, R. Laminar burning velocity and Markstein lengths of methane−air mixtures. *Combust. Flame* **2000**, *121* (1−2), 41−58.

(23) Kee, R. J.; Grcar, J. F.; Smooke, M. D.; Miller, J. A. *PREMIX, A FROTRAN Program for Modeling Steady Laminar One-Dimensional Premixed Flames*, SAND Report 85-8240; Sandia National Laboratories: U.S.A., 1985.

(24) Chaos, M.; Kazakov, A.; Zhao, Z. W.; Dryer, F. L. A high-temperature chemical kinetic model for primary reference fuels. *Int. J. Chem. Kinet.* **2007**, *39* (7), 399−414.

(25) Landau, L. On the theory of slow combustion. *Acta Physicochim. URSS* **1944**, *19* (1), 77−85.

(26) Darrieus, G. Propagation d'un front de flame. Unpublished work presented in Paris at La Technique Moderne, 1938, and Le Congrès de Méchanique Appliquée, 1945.

(27) Aung, K. T.; Hassan, M. I.; Faeth, G. M. Flame stretch interactions of laminar premixed hydrogen/air flames at normal temperature and pressure. *Combust. Flame* **1997**, *109* (1−2), 1−24.

(28) Searby, G.; Truffaut, J. M. Experimental studies of laminar flame instabilities. *Lect. Notes Phys.* **2001**, *567*, 159−181.

(29) Tang, C. L.; He, J. J.; Huang, Z. H.; Jin, C.; Wang, J. H.; Wang, X. B.; Miao, H. Y. Measurements of laminar burning velocities and Markstein lengths of propane−hydrogen−air mixtures at elevated pressures and temperatures. *Int. J. Hydrogen Energy* **2008**, *33* (23), 7274−7285.

(30) Law, C. K.; Jomaas, G.; Bechtold, J. K. Cellular instabilities of expanding hydrogen/propane spherical flames at elevated pressures: theory and experiment. *Proc. Combust. Inst.* **2005**, *30*, 159−167.

(31) Law, C. K.; Sung, C. J. Structure, aerodynamics, and geometry of premixed flamelets. *Prog. Energy Combust. Sci.* **2000**, *26* (4−6), 459−505.

(32) Gu, X. L.; Huang, Z. H.; Li, Q. Q.; Tang, C. L. Measurements of laminar burning velocities and Markstein lengths of *n*-butanol−air premixed mixtures at elevated temperatures and pressures. *Energy Fuels* **2009**, *23*, 4900−4907.

(33) Mounaim-Rousselle, C.; Broustail, G.; Seers, P.; Halter, F.; Moreac, G. Experimental determination of laminar burning velocity for butanol and ethanol *iso*-octane blends. *Fuel* **2011**, *90* (1), 1−6.

(34) Kumar, K.; Freeh, J. E.; Sung, C. J.; Huang, Y. Laminar flame speeds of preheated *iso*-octane/O_2/N_2 and *n*-heptane/O_2/N_2 mixtures. *J. Propul. Power* **2007**, *23*, 428−436.

(35) Bradley, D.; Gaskell, P. H.; Gu, X. J. Burning velocities, Markstein lengths, and flame quenching for spherical methane−air flames: A computational study. *Combust. Flame* **1996**, *104* (1−2), 176−198.

(36) Chen, Z.; Burke, M. P.; Ju, Y. Effects of compression and stretch on the determination of laminar flame speeds using propagating spherical flames. *Combust. Theory Modell.* **2009**, *13* (2), 343−364.

(37) Chen, Z.; Burke, M. P.; Ju, Y. G. Effects of Lewis number and ignition energy on the determination of laminar flame speed using propagating spherical flames. *Proc. Combust. Inst.* **2009**, *32*, 1253−1260.
(38) Tang, C. L.; Zheng, J. J.; Huang, Z. H.; Wang, J. H. Study on nitrogen diluted propane−air premixed flames at elevated pressures and temperatures. *Energy Convers. Manage.* **2010**, *51* (2), 288−295.
(39) Moss, J. T.; Berkowitz, A. M.; Oehlschlaeger, M. A.; Biet, J.; Warth, V.; Glaude, P. A.; Battin-Leclerc, F. An experimental and kinetic modeling study of the oxidation of the four isomers of butanol. *J. Phys. Chem. A* **2008**, *112* (43), 10843−10855.
(40) Wallner, T.; Miers, S. A.; McConnell, S. A comparison of ethanol and butanol as oxygenates using a direct-injection, spark-ignition engine. *J. Eng. Gas Turb. Power* **2009**, *131* (3), 032802.